Optimization of a High-Temperature High-Pressure Direct Wafer Bonding Process for III-V Semiconductors

Robert W. Martin, James K. Kozak, Kevin Anglin, William Goodhue
University of Massachusetts Lowell Photonics Center

Abstract: Direct wafer fusion of III-V semiconductors requires both high temperature and pressure to allow lattice mismatched bonding between molecules at the device interface. We use a carefully designed thermal expansion process consisting of a graphite chuck inside a hollow quartz tube to achieve this result, but improperly fused wafers and damage to the apparatus frequently occur. COMSOL's 2D and 3D structural mechanics modules are used to optimize the design geometry to guarantee a higher success rate of wafer fusion and promote the longevity of the bonding fixture.

Key Words: Wafer Fusion, Structural Mechanics

1. Introduction

There are many useful applications for single structure devices consisting of a fused pair of semiconductor wafers, including high efficiency MEMS devices, solar cells[1], light emitting diodes (LEDs) and vertical cavity surface emitting lasers (VCSELs)[2]. The production of these types of devices has been attempted by several methods, such as heteroepitaxial growth and direct wafer bonding, with varying degrees of success[3]. In heteroepitaxy, problems arise due to mismatched lattice structures. Specifically, this lattice mismatching leads to large problems with electrical conductance. Direct wafer bonding (DWB), which makes use of the Van der Waals interaction between the semiconductors' surfaces, requires extensive cleaning and annealing treatments. These annealing processes also often result in low conductance across the interface, which is highly undesirable. Other recent studies include DWB techniques that use a metallic film monolayer which provides low electrical resistance at the device interface and promotes successful bonding[4].

Wafer fusion of III-V semiconductors, as opposed to Si wafer bonding, requires high temperatures (>500 C) and high pressure in order to minimize deformities at the device interface. Our mechanism was originally modeled after the process developed by Liau *et al.*[5], in which a hollow quartz tube housing holds a pair of graphite half cylinders, between which the wafer pair is held (shown in Figure 1). Each wafer is first cleaned and aligned face to face in methanol before being loaded into the graphite halves. The entire fixture is then loaded into a tube furnace which is ramped slowly up to 700 °C. The high thermal expansion coefficient of the graphite causes it to rapidly expand, resulting in high, uniform pressure on each end of the wafer pair. Given that there is also high pressure exerted on the quartz tube by the graphite chucks, breaks in the tube and insufficient fusion of the wafers occur frequently. Since various devices using this fabrication technique require lapping, cleaving, and patterning post-bonding, maximizing the efficiency of the bonding mechanism would be an enabling technology. Here we study the stress and strain on the quartz tube, as well as the deformation and distribution of pressure on the wafer during this process, by varying the geometry of the bonding mechanism.

In this paper, three different models (A, B, and C) will be discussed extensively. The models contain several of the same elements. In each design, the quartz tube has an inner diameter of 6.52 cm. All of the models contain a single, 600 micron thick GaAs wafer. Each design also has a common top graphite piece of diameter Φ_{top}=6.21 cm. The final similarity is the length of the graphite chucks, which is 10.1cm in each model.

Model A is distinct from the others in that its bottom graphite piece has a diameter of Φ_{bot}=6.52 cm, which makes the bottom graphite chuck flush to the quartz tube along its curved surface. In model B, the diameter of the bottom graphite piece is decreased to Φ_{bot}=6.21 cm. Model C also has a smaller bottom graphite piece, Φ_{bot}=6.21 cm, and has a longer quartz tube as well (it is no longer flush with the ends of the graphite, but instead it is 1 cm longer on both sides).

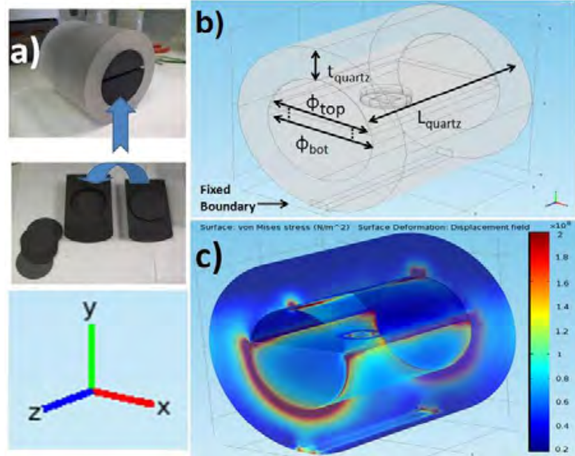

Figure 1: **a)** Photograph of experimental bonding apparatus **b)** Device schematic generated in COMSOL and detailed parameters. **c)** 3D COMSOL simulated von Mises stress of model A under external thermal heating.

2. Use of COMSOL Multiphysics

To improve bonding results using our fixture, it was necessary to explore many different geometric configurations, specifically by altering the radii of curvature of the graphite halves. To accomplish this, the Structural Mechanics module of COMSOL 4.0 was utilized. Both 2D and 3D models were created in order to highlight specific aspects of the process, both utilizing the thermal expansion feature. COMSOL's parametric solver also allowed an accurate simulation of the temperature ramping process for discrete temperature steps of 20 °C from 20 – 800 °C.

Figure 1 shows a schematic of our 3D COMSOL model, with the bottom of the quartz tube having a fixed constraint, and all other boundaries free to deform as the thermal expansion occurs. Post-processing visualization of the von Mises stress and deformation proved useful, as did 1-D line plots of the stress along the bottom half of the quartz tube, where breaks frequently occur. Surface plots of the 2D model allowed for studying wafer deformation during heating, the minimization of which would yield an improvement of wafer fusion.

3. Results and Analysis

Using COMSOL, three designs for the wafer fusion fixture were tested, each with a model for quartz tube thickness of 2 cm and a 3 cm.

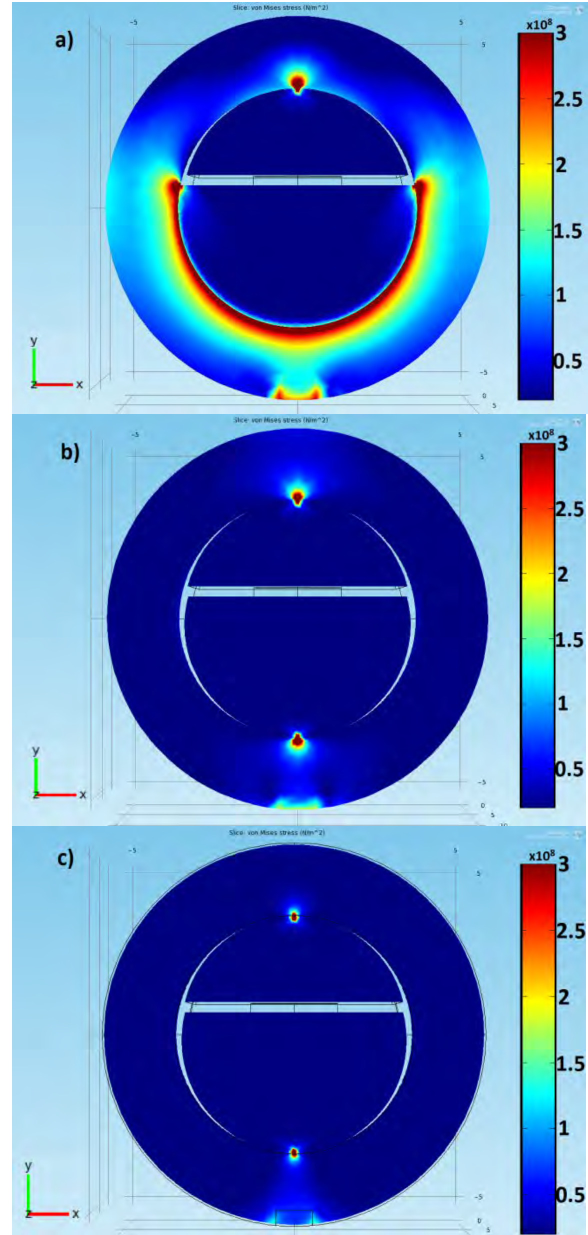

Figure 2: Cross sectional slices from 3D COMSOL simulations showing von Mises stress. Each slice is taken in the plane of the edge of the graphite. **a)** Model A (Φ_{bot}=6.52 cm, L_{quartz}=10.1cm), **b)** Model B (Φ_{bot}=6.21 cm, L_{quartz}=10.1 cm), and **c)** Model C (Φ_{bot}=6.21 cm, L_{quartz}=12.1 cm).

Each separate model was simulated at 700 °C, and the resulting von Mises stress and deformation data was used as the basis for our analysis. In every model, the top graphite piece has the same dimensions (Φ_{top}=6.21 cm), and likewise has a similar effect on the quartz tube during heating.

For models B and C, the top half of the model is identical to the bottom in regards to stress on the quartz tube.

Figure 2 depicts our results for the models with 2 cm quartz tube thickness. In model A, the stress from the bottom graphite piece is distributed along the entirety of the surface of the quartz it is in contact with. Additionally, cross sectional slices in the y-z plane (omitted) show that the stress continues along the length of the tube at a considerable level. This contrasts the other two models greatly. Model B shows a significantly reduced area of stress along the circumference of the glass tube from the graphite piece. This is consistent with the fact that, before thermal expansion, the graphite piece is only in contact with the quartz tube at one point in the x-y plane. In comparison to model A, the stress in the y-z direction also diminishes quickly as the distance from the edge of the tube increases. Model C differs further still from the other models. Though the bottom graphite piece also transfers stress at one point in the x-y plane, it has an extra 1 cm of quartz tubing extending beyond its end. Slices of the model in the y-z direction show the importance of the extra length of tubing. The stress in the quartz tube drops off quickly in the z direction. The y-z plane slices illustrate how this effectively increases the volume in which the stress can be absorbed. An analogy to this phenomenon would be pushing at the edge of a piece of paper will cause a rip, while pushing more towards the center with the same force would not cause any damage.

Similar differences exist among the three different designs in the models incorporating the 3 cm quartz tube thickness, in addition to a few new ones. Models A and B have the same stress along the inner boundary of the quartz tube in the 2 cm and 3 cm thick models. However, in model C, there is a significantly lower stress in the 3 cm thick model as compared to the 2 cm thick model. This is most likely another effect of having extra volume beyond the end of the graphite pieces.

While the stress in model A is lower than peak stresses in the other models, it is important to note the types of stresses the quartz tube is under. In model A, the graphite is pushing the quartz tube out in several directions, resulting in a tensile stress on the tube. In contrast, the bottom graphite pieces in models B and C are pushing down onto a single line along the length of the quartz tube. Because the stress is originating along this line and acting in only one direction, straight down into the quartz tube, it is a compressive stress. The design strengths for fused

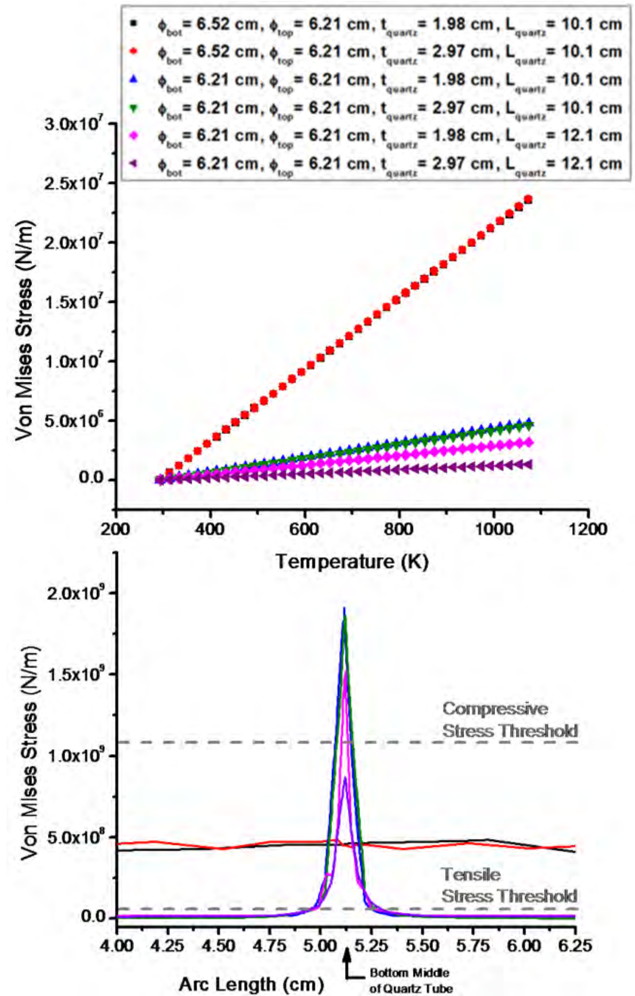

Figure 3: **a)** Averaged Von Mises Stress vs External Temperature along the inner boundary of the bottom of the quartz tube **b)** (same legend) Von Mises Stress vs. arc length along the bottom, inner boundary of the quartz tube. Horizontal lines are drawn at the tensile and compressive stress thresholds for fused quartz.

quartz, as given by the manufacturer, *Technical Glass*, are 4.9×10^7 Pa for tensile stress and at least 1.1×10^9 Pa for compressive stress. Figure 3 shows that model A, in both 2 cm and 3cm thicknesses, are beyond the design tensile strengths. However, the 3 cm thick model C is lower than the manufacturers design compressive and tensile stresses.

The objective of this process is to create a fused wafer pair. Preventing the quartz tube from breaking is necessary to provide an environment in which the wafers could fuse. However, even if the quartz tube survives the process, often the wafer pair does not fuse together properly. By altering the shape of the graphite pieces of the fixture, it was possible to change the magnitude and distribution of the stress on the wafer. From the simulations arose two distinct stress distributions for the wafer. These are shown in Figure 4.

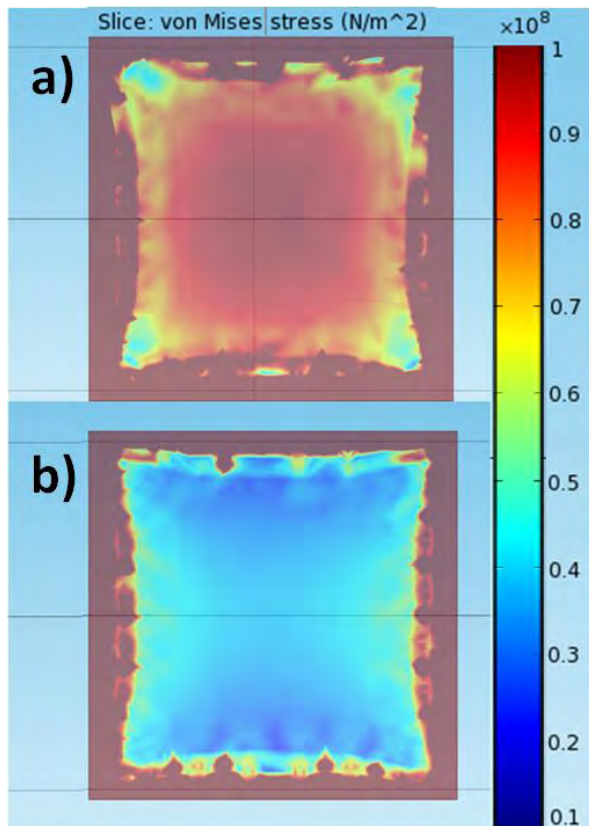

Figure 4: Cross sectional slices through the center of the wafer. **a)** von Mises stress in the wafer from model A. **b)** von Mises stress in the wafer from model B.

The stress from model A across the center of the wafer is more non-uniform, pointing to evidence for improper wafer fusion given this distribution of stress. Previously, the process has shown that bubbles form along the wafer-wafer interface and ripples develop along the surface of the wafers when the pressure on the wafer is not uniform. The wafer shown in Figure 4b is characteristic of both models B and C. The wafer is under more uniform stress in the center, and therefore would be less likely to resist bonding. The edges of the wafer are highly stressed in all scenarios, meaning that at least part of the wafers would become brittle and be lost during post-fusion lapping and processing no matter which design is used. To help prevent this, circular graphite shims are used to adjust the tightness of the wafers in the fixture. This helps adjust overall pressure on the wafers. COMSOL is needed to look at the distribution of stress in order to optimize the uniformity of the wafers.

It has also been found that the uniformity of the wafers and overall yield of the process may be further optimized with the use of additional shims. These shims are made from wafers of the same thickness as those being bonded. By placing these small shims around the perimeter of the wafer, the high lateral stress caused by the graphite deforming around the wafer can be lessened (see intensely red portions on the wafers' edges in Figure 4.).

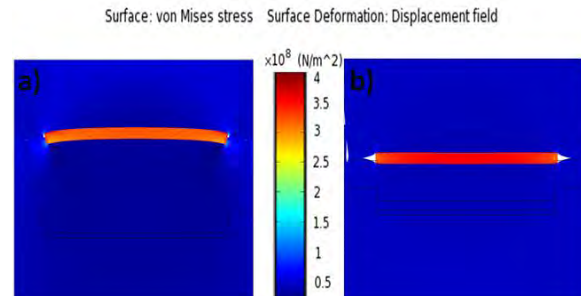

Figure 5. Von Mises Stress (center legend) for 2-D model (zoomed on wafer), also showing the displacement field Surface Deformation at a scale factor of 50 for **a)** Model A and **b)** Model B

Figure 5 shows 2D models of the deformation of the wafers. When viewed at a large scale factor (50), a significant difference between models A and B can be seen. The wafer in model A shows substantial bending, while model B shows no bending, even at this extreme scale factor. Although slight without being scaled, this bending of the wafers would cause inconsistent pressure at the interface and interfere with proper bonding of the wafers.

4. Conclusion

In conclusion, we have modeled the stresses and deformations caused by thermal expansion for our wafer bonding fixture when heated to 700 °C using COMSOL Multiphysics. By decreasing the radius of the mechanism's graphite chuck (from Φ_{bot}=6.52 cm to Φbot=6.21 cm), stress to the quartz tube has been minimized to prevent breaking, keeping it below the material's tensile and compressive stress thresholds. Elongation of the quartz tube by 2 cm (such that the graphite halves sit 1 cm inside of the edges) further adds to this prevention, by having the compressive stress not localized to the edge of the quartz tube. These apparatus design changes have improved our wafer bonding experimentally, yielding an enabling fabrication technique.

5. Acknowledgements

This work was supported by Hanscom Air Force Base AFRL/RYHC, contract no. FA8650-09-C-1653.

6. References

[1] P. R. Sharps, M. L. Timmons, J. S. Hills, and J. L. Gray, 26th IEEE
Photovoltaic Specialists Conference, 1997, p. 895.
[2] J. Jasinski and Z. Liliiental-Weber, Monostructure of GaAs/GaN interfaces produced by direct wafer fusion, *Applied Physics Letters*, **Vol. 81 Issue 17**, 3152-3153 (2002).
[3] U. Gosele and Q.-Y. Tong, Semiconductor Wafer Bonding, *Annual Reviews Materials Science*, **Vol. 28**, 215-241 (1998).
[4] I. Altfeder, Self-assembly of epitxial monolayers for vacuum wafer bonding, *Applied Physics Letters*, **Vol. 89, Issue 22**, 223127 (2006).
[5] Z. L. Liau and D. E. Mull, Wafer Fusion: A novel technique for optoelectronic device fabrication and monolithic integration, *Applied Physics Letters*, **Vol. 56 Issue 8**, p737-39 (1990).